Int. J. Electron. Commun. (AEÜ) 117 (2020) 153098

Contents lists available at ScienceDirect

International Journal of Electronics and Communications (AEÜ)

journal homepage: www.elsevier.com/locate/aeue

Regular paper

RCS reduction of reflectarray using new variable size FSS method

Sibel Ünaldı [a,*], Hande Bodur [b], Sibel Çimen [b], Gonca Çakır [b]

[a] Dept. of Control and Automation Engineering, Bilecik Şeyh Edebali University, Bilecik, Turkey
[b] Dept. of Electronics and Communications Engineering, Kocaeli University, Turkey

ARTICLE INFO

Article history:
Received 8 August 2019
Accepted 25 January 2020

Keywords:
Reflectarray antenna
Frequency Selective Surface
RCS

ABSTRACT

This study focuses on the reduction of the Radar Cross Section (RCS) for planar reflectarray antenna by using Frequency Selective Surface layers. For this study, a novel broadband reflectarray antenna is designed. The designed reflectarray antenna is composed of a broken circular ring and a cogwheel geometry. With variable size geometry, the proposed unit cell has more than 400° phase range which provides a broader bandwidth of the antenna. The RCS reduction of the reflectarray antenna is provided using variable size elements of the FSS technique and modification of reflectarray antenna ground plane. Therefore, the backscattering RCS of FSS backed modified reflectarray antenna is reduced up to 10 dB in the whole frequency band. This RCS reduction cost a reduction in terms of antenna gain level. The scattering characteristics, radiation patterns and RCS of both metallic grounded and FSS backed antennas are simulated and experimentally verified.

1. Introduction

Reflectarray antennas are combinations of phase shifting elements on a reflecting surface with an illuminating feed antenna. This type of antenna has several important features such as high gain, low cost, low profile, easy production, electronically beam direction ability [1–8]. Reflectarray antennas are usually used in military platforms because of their high gain features. Besides these advantages, these antennas have disadvantages on the RCS level of platforms and they increase the detectability [9–12]. Consequently, the reduced radar cross section of an antenna is a considerable factor for stealth technology due to the contribution of the antenna RCS [13].

In the literature, several methods are presented to enlighten this problem. These are listed as, reshaping [14,15], Electromagnetic Band Gap (EBG) [16,17], radar absorbing materials (RAM) for absorbing the EM wave and turn it into heat [18], passive cancellations or active cancellations [19] and FSS layers [20,21]. Particularly, the studies about RCS reduction of reflectarray antennas are limited. In [22], the RCS level of the reflectarray antenna is reduced only at out-of-band. In [23–26], FSS layers are used for RCS reduction of reflectarray antennas. All of these studies have RCS reduction only for incident wave impinging from normal direction ($\theta = 0^{\circ}$), not for oblique directions.

In this study, a new approach is introduced for RCS reduction of the reflectarray antenna. In this approach, a new variable size element FSS method is used. It is based on the reflection features of reflectarray. Reflectarray panels can generate a reflection beam in the desired direction. In this study, a novel broadband reflectarray antenna is designed. The designed reflectarray antenna is composed of a broken circular ring and a cogwheel geometry. With variable size geometry, the proposed unit cell has more than 400° phase range which provides a broader bandwidth of the antenna. Today periodic structures and antennas are used in many applications. The FSS is used in applications related to scattering electromagnetic waves while periodic structures such as metamaterials are used in applications [27,28] where specific constitutive parameters are realized.

The RCS reduction of the reflectarray antenna is provided using variable size elements of the FSS technique and modification of reflectarray antenna ground plane. The proposed broadband reflectarray antenna RCS level is reduced up to 10 dB in the whole frequency band (2–18 GHz). Naturally, the proposed antenna maximum gain value reduced from 21.23 dBi to 18.1 dBi. In this study, different from the literature, the RCS reduction of the reflectarray antenna, is also obtained for incident waves impinging from oblique directions, not for only normal direction. To show the validation of the proposed technique, metallic grounded and modified FSS layer backed reflectarray antennas are simulated and

* Corresponding author.
E-mail addresses: sibel.unaldi@bilecik.edu.tr (S. Ünaldı), hande.bodur@kocaeli.edu.tr (H. Bodur), sibelgunduz@kocaeli.edu.tr (S. Çimen), gonca@kocaeli.edu.tr (G. Çakır).

https://doi.org/10.1016/j.aeue.2020.153098
1434-8411/

measured due to obtain radiation patterns, gain and monostatic RCS characteristics.

2. Design of reflectarray

The geometry of the unit cell for the proposed reflectarray and FSS is demonstrated in Fig. 1(a) and side view of the unit cell is shown in Fig. 1(b). It is composed of a broken circular ring and a cogwheel. The presented geometry provides the desired phase characteristic. The design parameters of the proposed unit cell of the reflectarray antenna are chosen as ℓ = *variable*, $m = \ell/2 + 1$, $n = \ell/2$, $w = 0.4$, and ℓ is ranging from 3 mm to 7 mm. The overall dimension of the unit cell is $d = 16$ mm. There is a 5 mm air gap between the dielectric material and metallic ground. The presented metallic pattern of the unit cell geometry is printed on a dielectric substrate (Arlon Di880) with a $\varepsilon = 2.2$ relative permittivity and the thickness of h = 0.762 mm.

The phase characteristic has a significant effect on reflectarray performance. For this reason, it is important that the simulation of phase characteristics must be done properly. The unit cell reflection phase curves are obtained with the equivalent waveguide-approach in this study [26]. The periodic boundary conditions settings are used for normal wave incidence. At the boundary conditions, tangential component of incident Electric Field is set to Perfectly Magnetic Conductor (PMC) while the vertical wall is set to Perfectly Electric Conductor (PEC). The reflection coefficient (S_{11}) phase is evaluated as the reflected phase characteristic.

Reflection phase characteristic changing with ℓ for the proposed unit cell at 10.5–12 GHz is demonstrated in Fig. 2. By using variable size elements more than 400° phase range is obtained as seen in Fig. 2. Phase characteristics of the unit cell should be parallel to each other at various frequencies to obtain a wider operational band of reflectarray. Thereby, the reflection phase curve in Fig. 2 is the evidence of broadband reflectarray.

The phasing elements of the reflectarray that are fed by horn antenna reflect the EM waves to the backward. The EM wave will impinge on each unit cell with different phases because of positions of unit cells on reflectarray. The phase delay must be compensated due to direct the reflected EM wave towards the desired direction [29]. Therefore, the phase distribution of each unit cell of the reflectarray antenna placed at the x-y plane can be manipulated using the equations below.

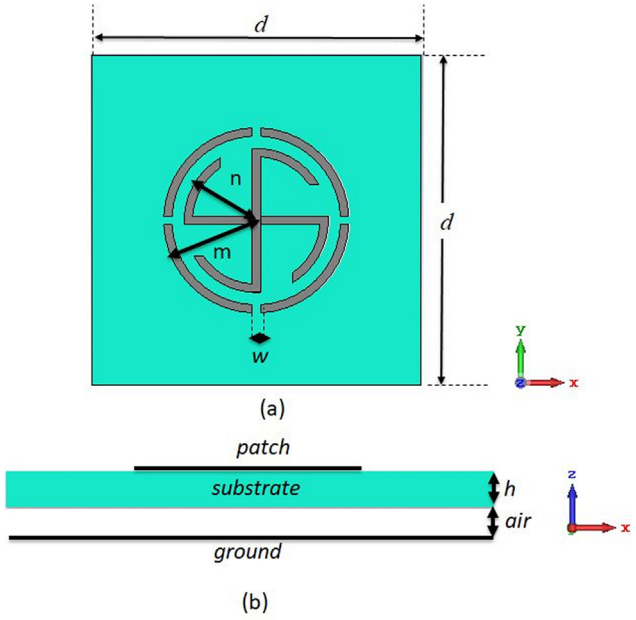

Fig. 1. (a) Top view of the unit cell, (b) Side view of the unit cell.

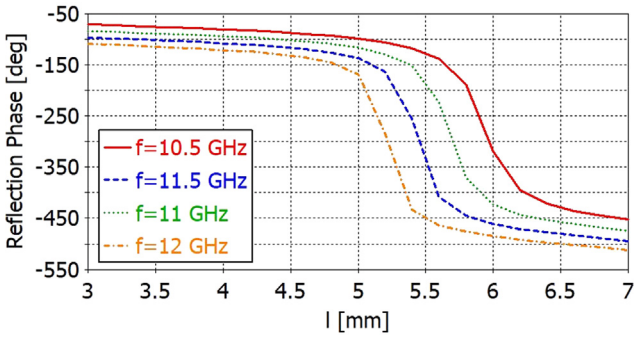

Fig. 2. Reflection phase curve.

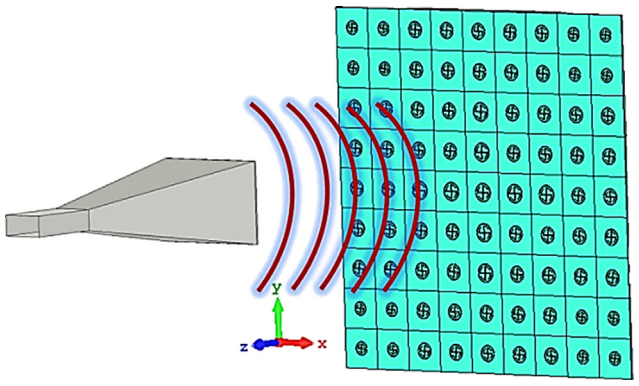

Fig. 3. Designed reflectarray and pyramidal horn antenna.

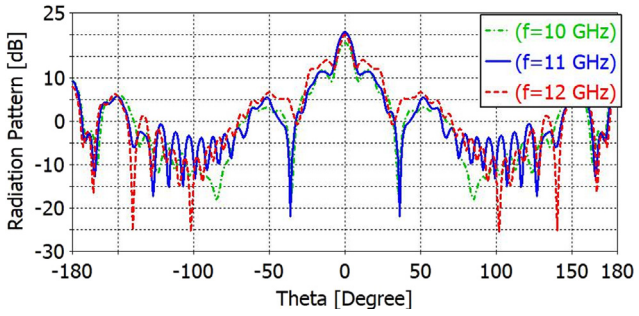

Fig. 4. Simulation results of radiation pattern for $\phi = 0°$ (E plane) at 10 GHz, 11 GHz and 12 GHz.

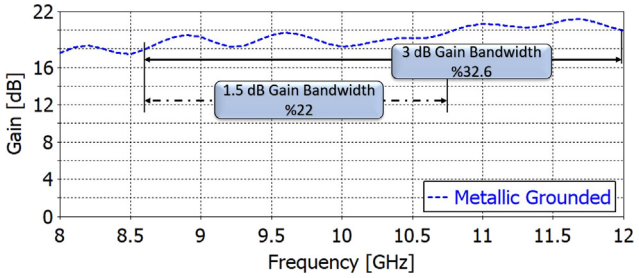

Fig. 5. Gain of designed reflectarray antenna.

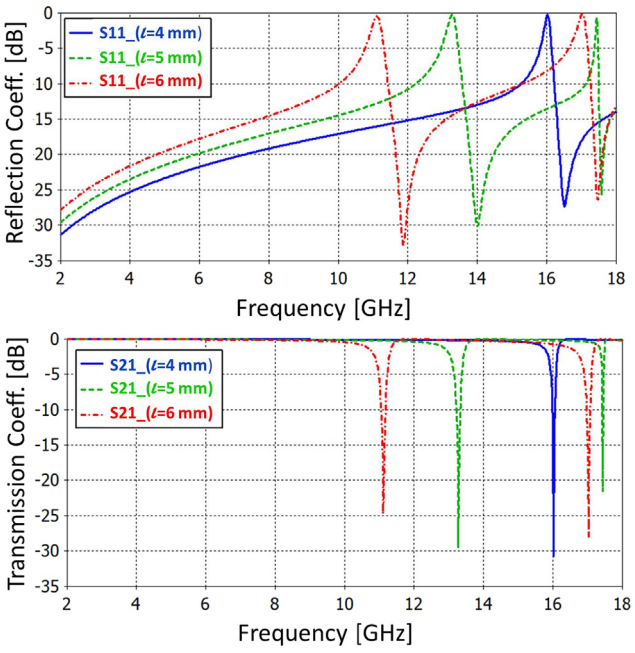

Fig. 6. Transmission and reflection characteristics for the different sized unit cell.

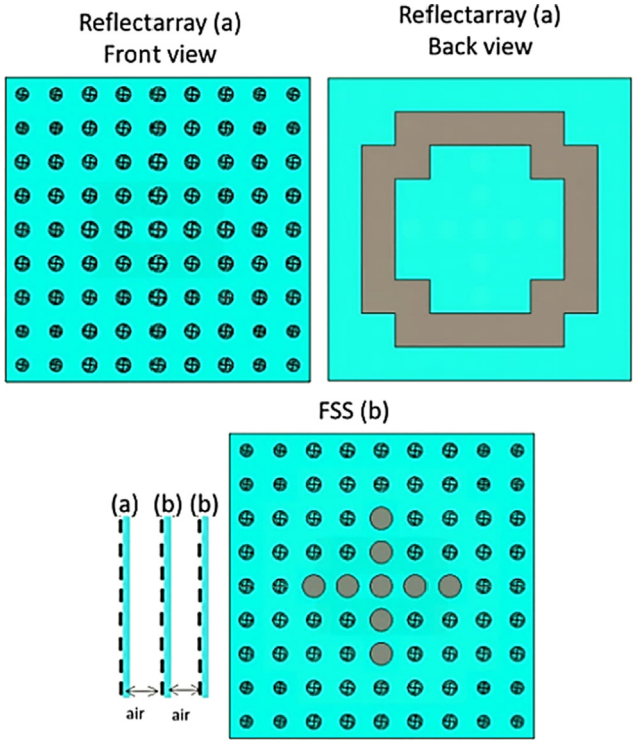

Fig. 7. FSS backed reflectarray antenna Configuration1.

$$\varphi_R(x_i, y_i) = k_0(d_i - (\cos\varphi_b x_i + \sin\varphi_b y_i)\sin\theta_b) \quad (1)$$

$$d_i = \sqrt{(x_i - x_f)^2 + (y_i - y_f)^2 + (z_i - z_f)^2} \quad (2)$$

Eq. (1) can be stated as Eq. (3) which determines the required phase distribution of each unit cell if the maximum radiation is oriented along to z-axis and center-fed configuration is applied.

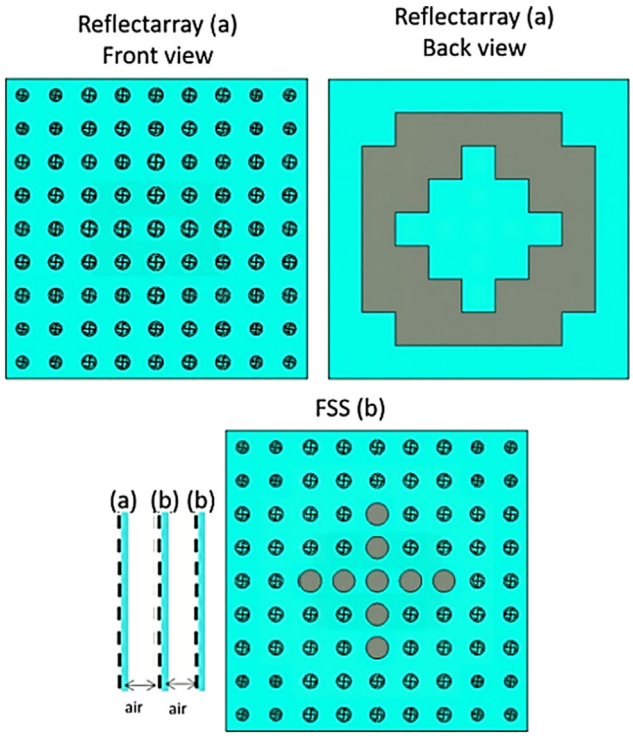

Fig. 8. FSS backed reflectarray antenna Configuration2.

$$\varphi_R(x_i, y_i) = k_0 d_i \quad (3)$$

In these equations, $\varphi_R(x_i, y_i)$ is the phase shift of i^{th} element, k_0 is the free space propagation constant, d_i gives the distance between the source and $(x_i, y_i)^{th}$ element, x_i and y_i are the coordinates of the i^{th} element of the reflectarray antenna and θ_b, φ_b indicate the desired beam direction [30]. x_f, y_f and z_f are the coordinates of the source antenna. Thus, the size of the reflectarray elements can be determined. To this end, the required phase delay of each element can be calculated using Eqs. (1) and (2).

The focal distance (F) is defined as the distance between the surface of the reflectarray and horn antenna aperture and F is set as 198 mm. The proposed reflectarray is fed by a linearly polarized horn antenna. At the focal distance (F) pyramidal horn antenna is placed the center of the reflectarray. The feeder pyramidal horn antenna has 3 dB beamwidth approximately 30°. A 9 × 9 elements

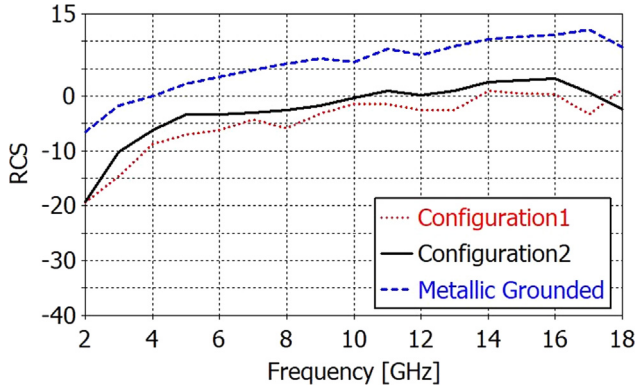

Fig. 9. Simulation results of monostatic RCS for the metallic grounded antenna and designed configurations.

reflectarray antenna which is used for RCS reduction has 135 mm × 135 mm overall dimensions in x and y directions. The reflectarray antenna is illustrated in Fig. 3. The proposed reflectarray antenna is simulated and far field radiation patterns, gain versus frequency characteristics are achieved.

The simulations of the reflectarray antenna are done by time domain solver of the CST Microwave Studio. Also, in the simulation the symmetry planes are defined to save time. Afterward, the gain and far field radiation patterns are obtained to validate the designed reflectarray antenna. In Fig. 4, the radiation patterns in E-plane at 10 GHz, 11 GHz and 12 GHz frequencies are given. The maximum gain of the reflectarray antenna is 21.23 dBi and it has 22% 1.5-dB (8.63 GHz-10.7 GHz) and 32.6% 3-dB gain bandwidth (between 8.63 GHz and 12 GHz) as shown in Fig. 5.

3. FSS backed reflectarray design and simulations

Planar metallic grounded antennas like reflectarray antennas have considerable RCS levels. For this reason, a new type of FSS reflector is designed to reduce the RCS level. In this method, variable size FSS unit cells are used in the reflector plane. In this manner, it is different from traditional FSS layers. The unit cell geometry of FSS is the same as reflectarray unit cell geometry

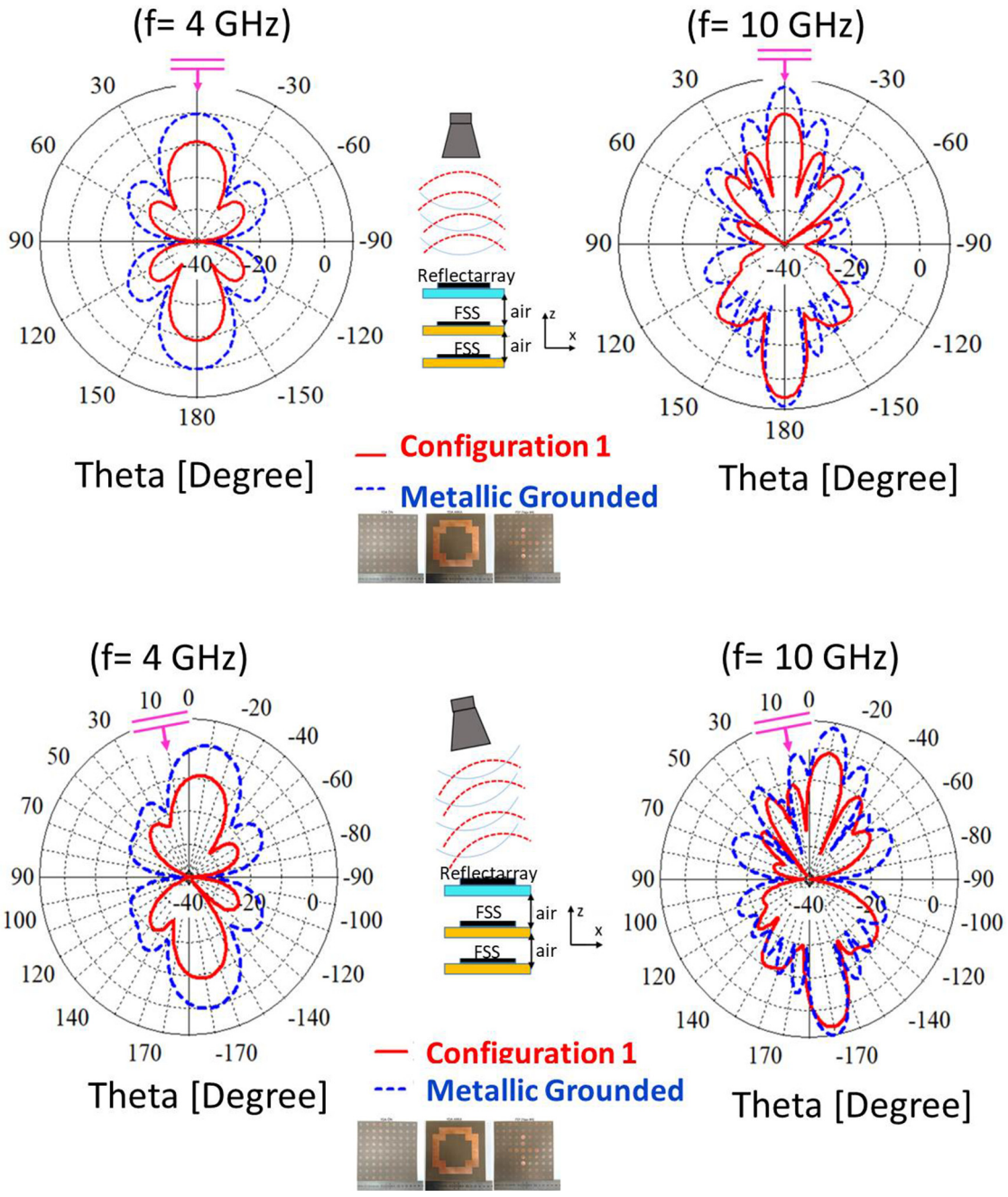

Fig. 10. Backscattering pattern of metallic grounded and Configuration1 reflectarray at 4 GHz and 10 GHz for $\theta = 0^{\circ}$ and $\theta = 10^{o}$, respectively.

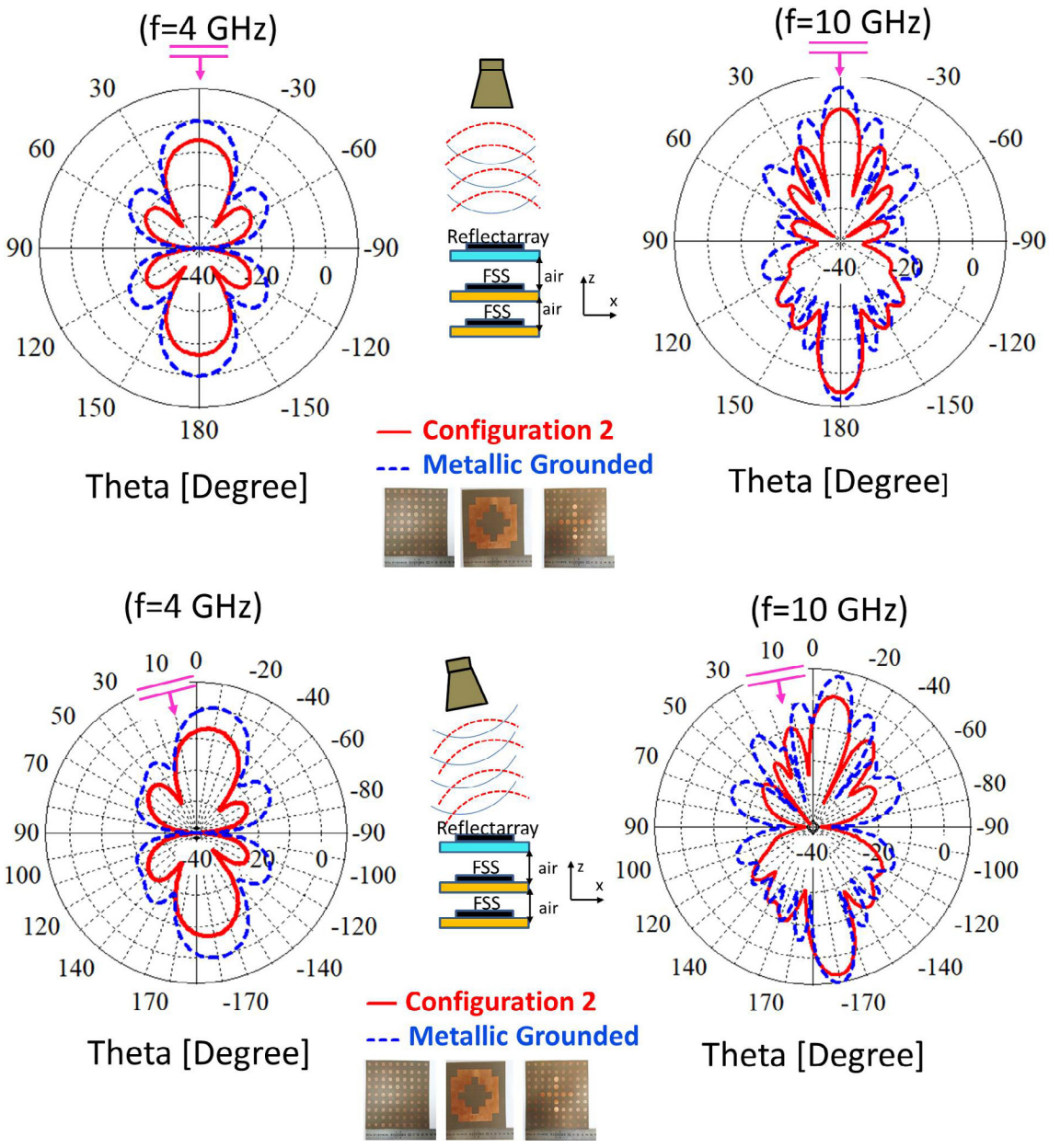

Fig. 11. Backscattering pattern of metallic grounded and Configuration2 reflectarray at 4 GHz and 10 GHz for $\theta = 0^{\circ}$ and $\theta = 10^{\circ}$, respectively.

(Fig. 1a). As seen from Fig. 6b, the metallic circular patches are added to the proposed FSS layer with different sizes. The metallic circular patches improve the RCS reduction. The designed double layer FSS is settled back of the reflectarray. The FSS layers used in the design are identical. The double layer FSS structure is preferred to obtain an improvement of the gain characteristic compared to the single layer FSS. The unit cell analyzes of the FSS structure in this design were performed for 3 different sized unit cells ("ℓ" parameter of the design is used as 4 mm, 5 mm and 6 mm) used in the structure. The obtained transmission and reflection characteristics for the 3 different sized unit cells are shown in Fig. 6. As seen in Fig. 6, the reflection coefficients of the unit cells at the range of 2–18 GHz band are quite low. This shows that the structure does not reflect the incoming EM wave back, it transmits to forward. Thus, RCS is reduced at the 2–18 GHz frequency band by using different sizes of unit cells.

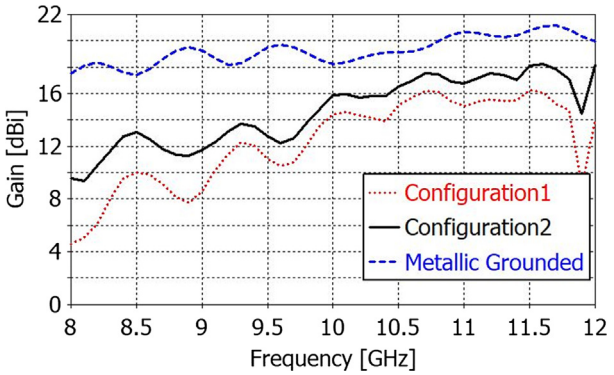

Fig. 12. Simulation results of gain for the metallic grounded antenna and designed configurations.

The proposed reflectarray ground plane is also modified with two configurations as seen in Figs. 7 and 8. The designed configurations consist of the same double layer FSSs behind the reflectarray and but have different metallic patches on the back surface of reflectarray. There is an air layer (5 mm) between dielectric substrates of the FSS layers.

Therefore, the RCS performances of proposed configurations are carried out. For this reason, metallic grounded and double layer FSS backed reflectarray antennas are simulated and monostatic RCSs are obtained as in Fig. 9. The monostatic RCS simulations are obtained for a plane wave normally, impinging with TE polarization. It is clearly seen from Fig. 9, Configuration1 and 2 provide RCS reduction in the whole frequency band. The main reason for using the 2–18 GHz frequency range in RCS graphics is to show that the antenna is also reduced RCS outside the operating frequency range (designed reflectarray operates at the range of 8–12 GHz). As Configuration1 provides more than 10 dB RCS reduction, Configuration2 provides about 8 dB reduction in 2–18 GHz frequency band.

In literature, RCS reduction is obtained only for incident wave impinging from normal direction ($\theta = 0^o$), not for oblique directions. In this study, different from the literature, the RCS reduction of the reflectarray antenna, is also obtained for incident wave impinging from oblique directions. The simulation

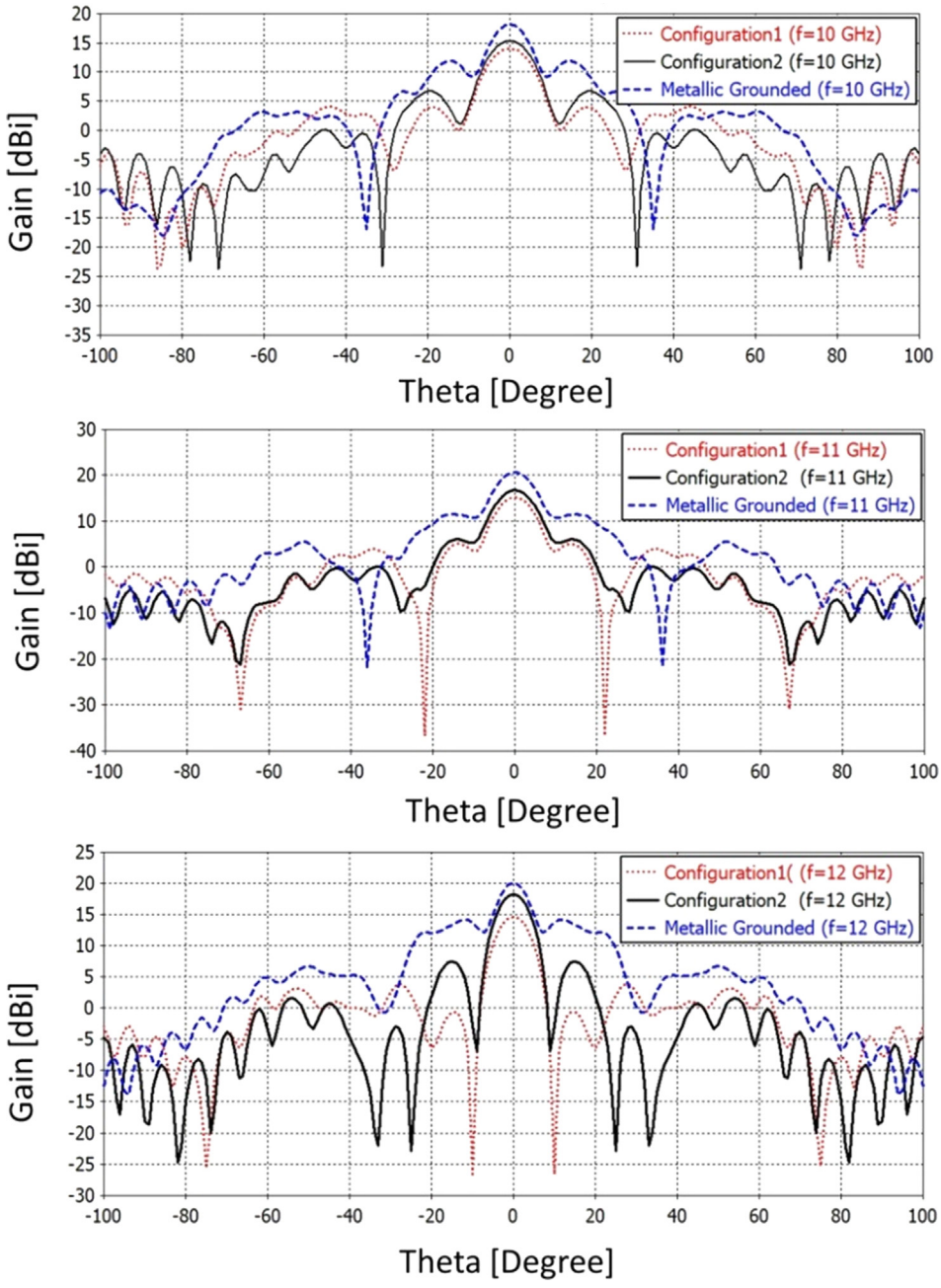

Fig. 13. Simulated radiation patterns in E plane at different frequencies for metallic grounded, Configuration1 and Configuration2 structures.

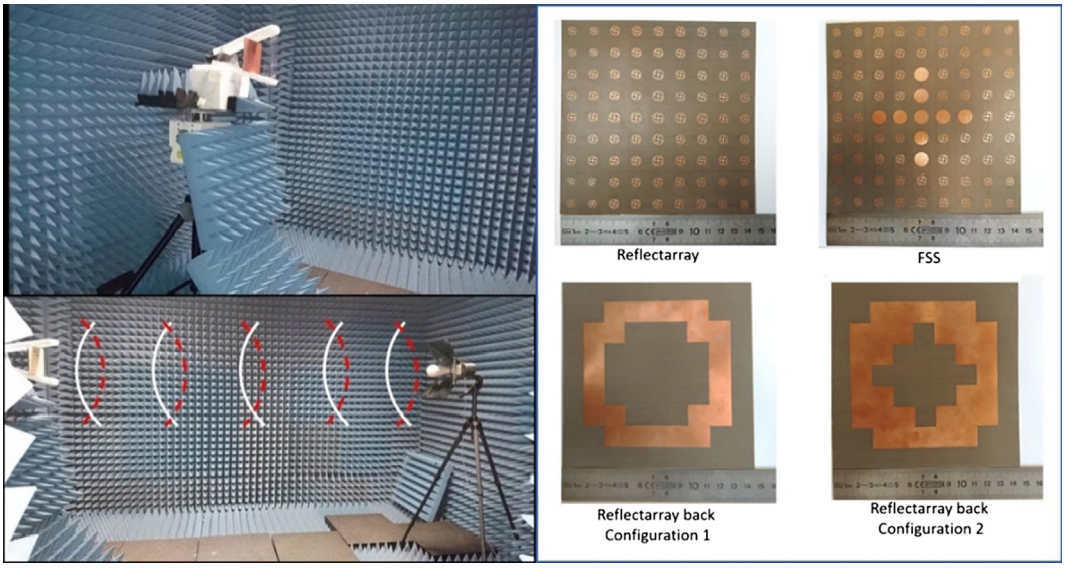

Fig. 14. Photograph of measurement set up and fabricated Configuration 1 and 2.

results of monostatic RCS versus theta is given in Figs. 10 and 11. For Configuration1 and Configuration2, respectively. Therefore, RCS reduction is achieved also at the oblique incidence of the wave.

In Fig. 12, simulation results for the gain of the metallic grounded reflectarray antenna and proposed configurations are compared. As seen from the figure, the gain is reduced for Configuration1 and 2. The gain versus frequency characteristic is obtained at $\theta = 0°$, $\phi = 0°$ direction. In this direction, EM wave scatters towards backside of the structure. Naturally, the proposed antenna maximum gain value reduced from 21.23 dBi to 18.1 dBi.

Also, in Fig. 13 there is a comparison of the simulated radiation patterns for Configuration1, Configuration2 and metallic grounded reflectarray at different frequencies (f = 10 GHz, f = 11 GHz, and f = 12 GHz).

4. Fabrication and measurements

The designed and simulated Configuration1, Configuration2 and original reflectarray antenna are fabricated. Photos of the measurement set-up and fabricated prototypes of the reflectarray, Configuration1 and Configuration2 are shown in Fig. 14. For measurement, a pyramidal horn antenna is used for center fed configuration.

Horn antenna is located at F = 198 mm away to array surface. Radiation pattern and RCS measurements were performed in a whole anechoic chamber. The 3-m anechoic chamber has a 900 MHz–20 GHz frequency range. The measurements are done with a transmitting horn antenna (Model: De0530 Diamond Engineering) and Rohde & Schwarz ZVB 20 VNA (Vector Network Analyzer) with the low-loss coaxial cable.

In Figs. 15 and 16, the radiation performances are presented. The simulated and measured gains for Configuration1 and Configuration2 are given in Fig. 15. In Fig. 16, there are simulated and measured radiation patterns of Configuration1 and Configuration2 for frequencies of 8.5, 9.2 and 11.3 GHz in the E-plane. Due to the measurement set up imperfection, scattering from feeder mount and fabrication errors in structure, Figs. 15 and 16 show some discrepancy between the measurement results and the simulation

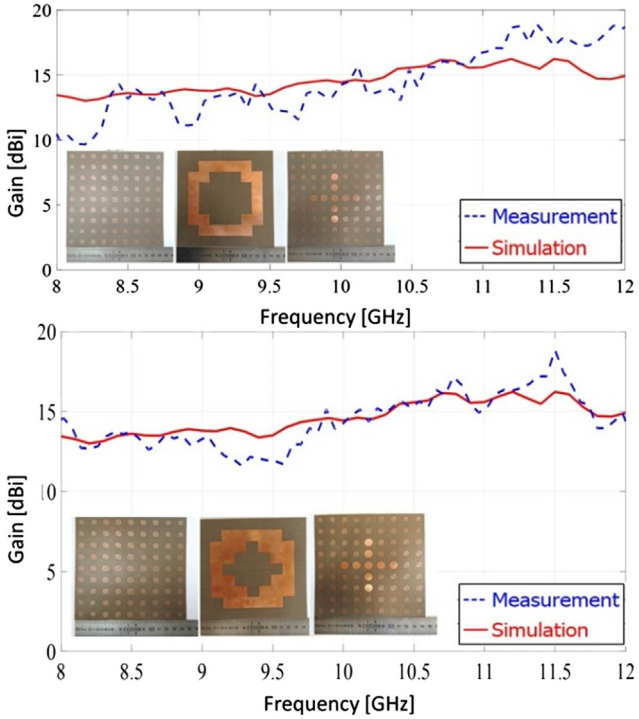

Fig. 15. Measured and simulated gains for Configuration1 and 2 structures.

results. Besides this, measured and simulated results are in good agreement.

After the radiation performance measurements, the monostatic RCS measurements were performed in a whole anechoic chamber. For the RCS measurements and simulations, the incoming and reflected electric field is taken parallel to the x-axis. Besides this, the propagation direction of the incoming wave is parallel to the z-axis. In Figs. 17 and 18 there are obtained RCS results both for Reflectarray, Configuration1 and 2. It was observed that the measurement results confirmed the simulated results.

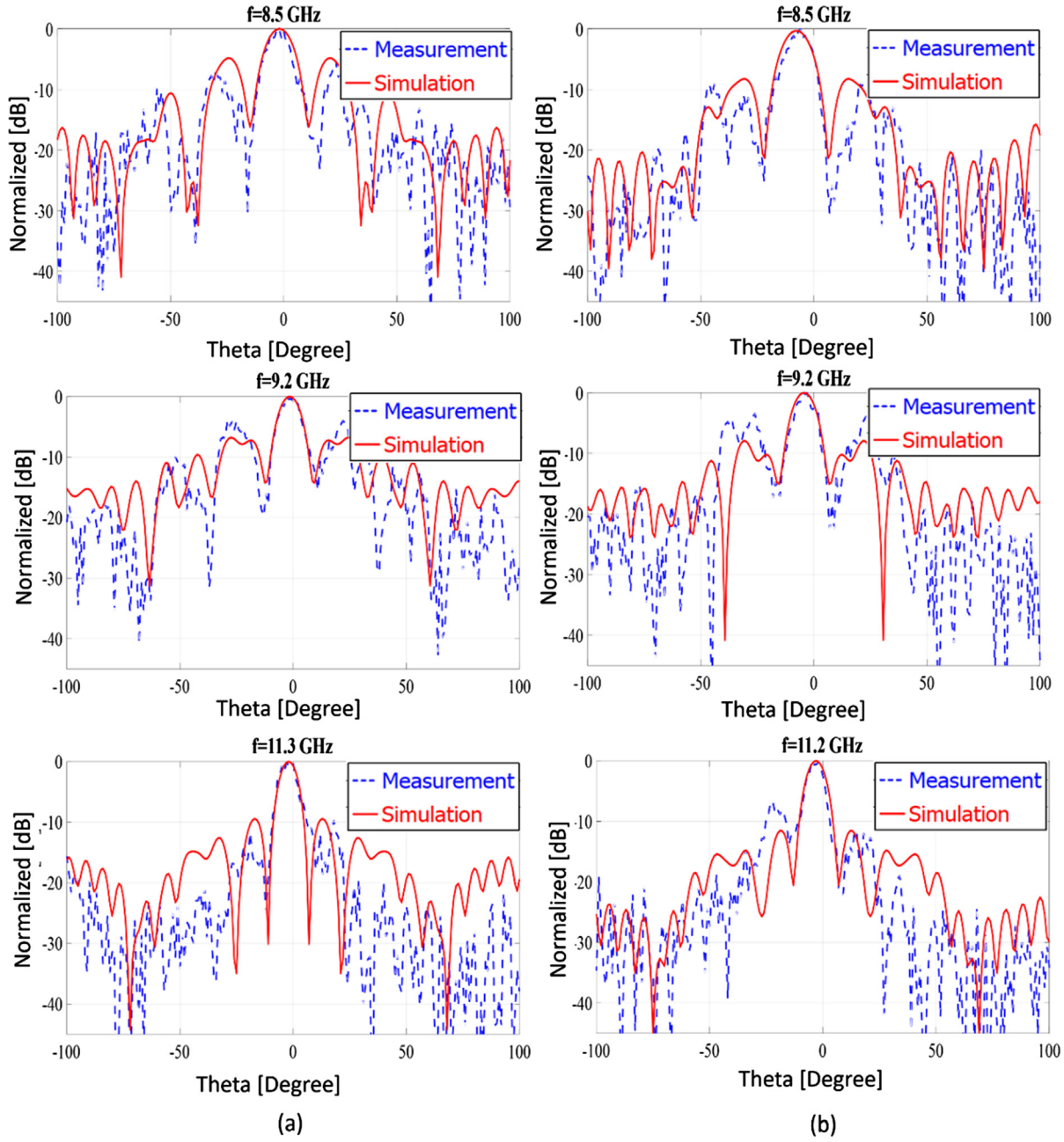

Fig. 16. Measured and simulated radiation patterns in E plane at different frequencies for (a) Configuration1 and (b) Configuration2.

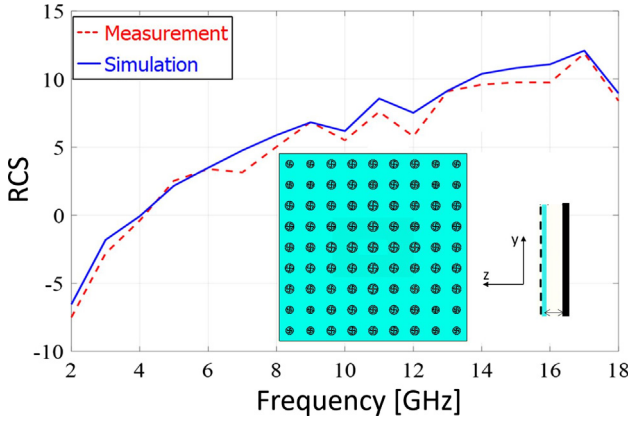

Fig. 17. Measured and simulated monostatic RCS for the Reflectarray.

5. Conclusion

In this study, a broadband reflectarray antenna with low RCS level is presented. The RCS reduction is obtained with double layer FSS which have variable sized unit cell elements. The proposed reflectarray antenna with metallic grounded and FSS backed are designed, simulated and fabricated. The reflectarray configurations are performed using CST Microwave Studio. To verify the validity of the proposed method, designed structures are fabricated and measured. The measurement and simulation results for designed FSS grounded reflectarray shows decreased RCS level effectively almost in the whole band (2–18 GHz). Thereby, good agreements are obtained between simulations and measurement results for both configurations. Therefore, the proposed method can be used in the studies aimed at RCS reductions.

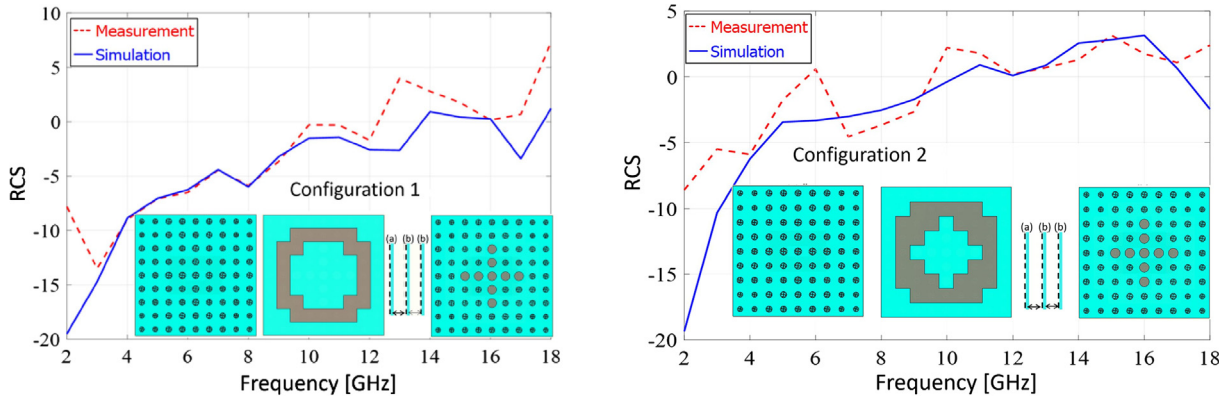

Fig. 18. Measured and simulated monostatic RCS for the Configuration1 and Configuration2.

Declaration of Competing Interest

The authors declare that they have no known competing financial interests or personal relationships that could have appeared to influence the work reported in this paper.

Acknowledgments

The authors wish to acknowledge the assistance and support of The Scientific and Technological Research Council of Turkey (TUBITAK) for supporting this work (Project No: 114E500).

References

[1] Huang J, Encinar JA. Reflectarray antennas. Piscataway NJ, USA: IEEE Press/Wiley; 2008. https://doi.org/10.1002/9780470178775.
[2] Carrasco E, Barba M, Encinar JA, Arrebola M. Design manufacture and test of a low-cost shaped-beam reflectarray using a single layer of varying-sized printed dipoles. IEEE Trans Anten Propagat 2013;61:3077–85. https://doi.org/10.1109/TAP.2013.2254431.
[3] Tienda C, Arrebola M, Encinar JA, Toso G. Analysis of a dual-reflectarray antenna. IET Microw Anten Propag 2011;5(13):1636–45;
Nadaud K, Gillard R, Fourn E, Gundel HW. Equivalent circuit of a reconfigurable triple-slot reflectarray cell. IET Microw Anten Propag 2016;10(10):1080–6. https://doi.org/10.1049/iet-map.2010.0444.
[4] Nadaud K, Gillard R, Fourn E, Gundel HW. 'Equivalent circuit of a reconfigurable triple-slot reflectarray cell. IET Microw Anten Propag 2016;10 (10):1080–6. https://doi.org/10.1049/iet-map.2015.0378.
[5] Edalati A, Sarabandi K. Reflectarray antenna based on grounded loop-wire miniaturised-element frequency selective surfaces. IET Microw Anten Propag 2014;8(12):973–9. https://doi.org/10.1049/iet-map.2013.0432.
[6] Chaharmir MR, Shaker J, Legay H. Dual-band Ka/X reflectarray with broadband loop elements. IET Microw Anten Propag 2010;4(2):225–31. https://doi.org/10.1049/iet-map.2008.0369.
[7] Wang H, Li Y, Chen H, Shen Y, Yang Z, Wang J, et al. Spin-to-orbital angular momentum conversion with quasi-continuous spatial phase response. Adv Opt Meter 2019;7:no.24. https://doi.org/10.1002/adom.201901188.
[8] Wang H, Li Y, Han Y, Fan Y, Sui S, Chen H, et al. Vortex beam generated by circular-polarized metasurface reflector antenna. J Phys D Appl Phys 2019;52 (25). https://doi.org/10.1088/1361-6463/ab1742.
[9] Euler M, Fusco VF. RCS control using cascaded circularly polarized frequency selective surfaces and an AMC structure as a switchable twist polarizer. Microw Opt Technol Lett 2010;52:577–80. https://doi.org/10.1002/mop.24979.
[10] White MO. Radar cross-section: measurement, prediction and control. Electron Commun Eng J 1998;10:169–80. https://doi.org/10.1049/ecej:19980403.
[11] Ren L-S, Jiao Y-C, Zhao J-J, Li F. RCS reduction for a FSS-backed reflectarray using a ring element. Prog Electromag Res Letters 2011;26:115–23. https://doi.org/10.2528/PIERL11071201.
[12] Y. Ruan, Radar cross section and stealth technology. Beijing, China: Nat. Defense Ind.; 1998.
[13] Wang H, Huang J, Wang H, Li Y, Sui S, Li W, et al. Chaos-based coding metasurface for radar cross-section reduction. J Phys D Appl Phys 2019;52: no.40. https://doi.org/10.1088/1361-6463/ab2dc6.
[14] Amutha M, Karthipan R. UWB radar cross section reduction in a compact antipodal Vivaldi antenna. AEU - Int J Electron Commun 2019;99:369–75.
[15] Tayyab AK, Jianxing L, Zhiyuan L, Muhammad A, Juan C, Anxue Z. Design of a Vivaldi antenna with wideband reduced radar cross section. AEU - Int J Electron Commun 2018;95:47–51.
[16] Yang F, Rahmat-Samii Y. Microstrip antennas integrated with electromagnetic band-gap (EBG) structures: A low mutual coupling design for array applications. IEEE Anten Wirel Propag Lett 2017;51(10):1631–4. https://doi.org/10.1109/TAP.2003.817983.
[17] Dhawan S, Viranjay MS. An analysis of RCS for dual-band slotted patch antenna with a thin dielectric using shorted stubs metamaterial absorber. AEU - Int J Electron Commun 2018;90:53–62.
[18] Han Z-J, Song W, Sheng X-Q. Gain enhancement and RCS reduction for patch antenna by using polarization-dependent EBG surface. IEEE Anten Wirel Propag Lett 2017;16:1631–4. https://doi.org/10.1109/LAWP.2017.2658195.
[19] Gao Q, Yin Y, Yan D-B, Yuan NC. Application of metamaterials to ultra-thin radar-absorbing material design. Electron Lett 2005;41(17):936–7. https://doi.org/10.1049/el:20051239.
[20] Knott EF, Shaeffer JF, Tuley MT. Radar cross section. 2nd ed. Raleigh (NC, USA): SciTech; 2004. ISBN 9781891121258.
[21] Genovesi S, Costa F, Monorchio A. Low-profile array with reduced radar cross section by using hybrid frequency selective surfaces. IEEE Trans Anten Propag May 2012;60(5):2327–35. https://doi.org/10.1109/TAP.2012.2189701.
[22] Misran N, Cahill R, Fusco VF. RCS reduction technique for reflectarray antennas. Electron Lett 2003;39(23):1630–1. https://doi.org/10.1049/el:20031070.
[23] Li H, Wang B-Z, Zheng G, Shao W, Guo L. A refectarray antenna backed on FSS for low RCS and high radiation performances. Prog Electromag Res C 2010;15:145–55. https://doi.org/10.2528/PIERC10070303.
[24] Li L, Chen Q, Yuan Q-W, Sawaya K, Maruyama T, Furuno T, et al. Frequency selective refectarray using crossed-dipole elements with square loops for wireless communication applications. IEEE Trans Anten Propag 2011;59 (1):89–99. https://doi.org/10.1109/TAP.2010.2090455.
[25] Bodur, H., Çimen, S., Çakir, G., Ünaldi, S. A novel reflecarray antenna backed with double layer FSS for RCS reduction. In Proceedings of the international applied computational electromagnetics society symposium (ACES). Florence (Italy); March 2017. https://doi.org/10.23919/ROPACES.2017.7916046.
[26] Albanı M, et al. Concepts for polarising sheets dual-gridded reflectors for circular polarisation. In Proceedings of the 20th international conference on applied electromagnetics and communications (ICECom), Dubrovnik (Croatia); Sep 2010, p. 1–4.
[27] Liu Feng, Guo Jiayin, Zhao Luyu, Huang Guan-Long, Li Yingsong, Yin Yingzeng. Dual-band metasurface-based decoupling method for two closely packed dual-band antennas. IEEE Trans Anten Propagat 2020;68(1):552–7. , https://ieeexplore.ieee.org/document/8839702/. https://doi.org/10.1109/TAP.810.1109/TAP.2019.2940316.
[28] Shengyuan L, Yingsong L, Yinfeng X, Liang Z. A low mutual coupling antenna array with gain enhancement using metamaterial loading and neutralization line structure. ACES J 2019;34(3):411–8.
[29] Bodur H, Ünaldi S, Çimen S, Çakir G. Broadband single-layer reflectarray antenna for X-band applications. IET Microw Anten Propag 2018;12 (10):1609–12. https://doi.org/10.1049/iet-map.2017.0270.
[30] Carrasco E, Encinar JA, Barba M. Bandwidth improvement in large reflectarrays by using true-time delay. IEEE Trans Anten Propagat 2008;56(8):2496–503.